Ionic current through a nanopore three nanometers in diameter

Yanyan Ge,[1] Dongyan Xu,[2] Juekuan Yang,[1,2] Yunfei Chen,[1,*,†] and Deyu Li[2,*,‡]
[1]*Jiangsu Key Laboratory for Design and Manufacture of Micro-Nano Biomedical Instruments and China Education Council Key Laboratory of MEMS, School of Mechanical Engineering, Southeast University, Nanjing 210096, People's Republic of China*
[2]*Department of Mechanical Engineering, Vanderbilt University, Nashville, Tennessee 37235, USA*
(Received 12 March 2009; revised manuscript received 22 May 2009; published 18 August 2009)

Ionic current through a 3 nm in diameter nanopore has been investigated using molecular dynamics. Results indicate that the ionic current increases linearly as the electrolyte concentration increases from 0.4 to 0.9 M, beyond which the ionic current increases at a slower rate. In contradiction to the expectation that higher surface charge density will lead to more ions in the nanopore, and therefore, higher ionic current, the ionic current shows an increase-decrease profile as the surface charge density increases. These unusual observations are attributed to the fact that ions close to the wall experience large viscous force, leading to low mobility.

DOI: 10.1103/PhysRevE.80.021918 PACS number(s): 87.10.−e, 47.61.Fg

I. INTRODUCTION

Nanoscale Coulter-type sensors, such as those based on naturally occurring protein nanopores or man-made inorganic nanopores/nanochannels with dimensions comparable to the size of single molecules or the Debye length, have attracted significant attention over the past decade because of their ability to detect single molecules [1–5]. These nanoscale Coulter counters rely on sensing the ionic current through the nanopore and its modulation from the translocation of individual nanoparticles or single molecules to detect and interrogate the properties of the nanoparticles or molecules. The baseline ionic current itself, which is determined by the pore size, the electrolyte concentration, the applied electric field, and the surface properties of the nanopore, is of significant interest because it discloses many unique phenomena occurring in the nanochannels. In addition, the stability and noise of the baseline ionic current determine the sensitivity of the nanoscale Coulter-type devices. Several experimental studies were carried out recently to understand the ionic current through nanochannels. Stein *et al.* [6] measured the electrical conductance of silica nanochannels filled with different concentration KCl buffered solutions. Their results indicated that at low concentration, the electrical conductance was determined solely by the surface charge, independent of the salt concentration. Daiguji *et al.* [7] first reported theoretically the possibility of creating a unipolar solution of counter ions in a 30 nm in diameter silica nanotubes and using a gate electrode to modulate the ionic current through the nanotubes. Later, Karnik *et al.* [8] experimentally observed the modulation of the electrical resistance through both ~50 nm in diameter nanotubes and 40 nm high, 1 μm wide nanoslits by applying a gate potential. Schoch and Renaud [9] measured and modeled the electrical conductance of an electrolyte-filled nanoslit of 50 nm in height. Their results indicated that at low-salt concentrations, the electrical conductance was dominated by the effective surface charge density, which could be regulated by the pH and external gate potential. To date, all studies indicate that the ionic current at low concentrations (below about 0.1 M) is determined by the surface charge density, while at higher concentrations, the ionic current can be estimated based on the bulk electrolyte concentration and the size of the nanopore. However, all previous research really focused on the effects of overlapped electric double layers without paying much attention to the ionic transport through nanopores for high-concentration electrolytes with nonoverlapped double layers. Therefore, the ionic current data for high-concentration electrolyte through nanochannels are limited and not systematic. Molecular dynamics (MD) simulations can provide a detailed molecular description of the interactions between the solvated ions and the solid surface, offering a valuable tool for studying the electrolyte behavior in highly confined nanochannels. With the space positions and the velocities of all particles at different time solved from the Newton's second law, statistical parameters can be obtained from the simulation. In recent years, with the rapid increase in the computational power, MD method has become an important tool to study the electrolyte behavior in the nanochannels [10–23].

In this paper, we report on a MD study of ionic current through a 3 nm in diameter nanopore. Results indicate that the ionic current increases linearly as the electrolyte concentration increases from 0.4 M to about 0.9 M, beyond which the ionic current still increases but at a rate significantly lower than linear. In addition, for the same electrolyte concentration, the ionic current follows an increase-decrease profile as the surface charge density increases, which is contradictory to the anticipation that higher surface charge density will lead to more mobile ions in the nanopore, and therefore, higher ionic current. Further examination of the ion distribution and velocity profile discloses that at high-electrolyte concentrations or high-surface charge densities, more counter ions are in the near wall region, experiencing larger viscous force, which could explain the slower increase rate at high-electrolyte concentrations and the ionic current reduction at high-surface charge densities.

*Corresponding authors.
†yunfeichen@seu.edu.cn
‡deyu.li@vanderbilt.edu

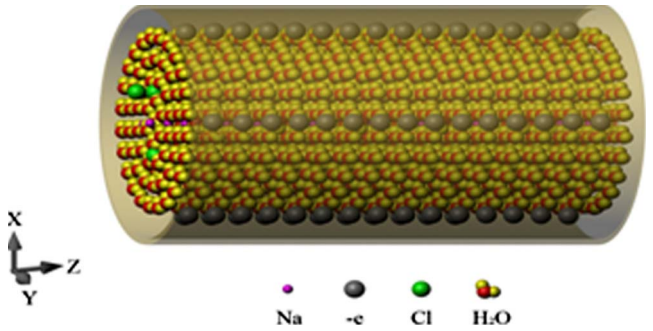

FIG. 1. (Color online) A schematic diagram of the nanopore model. Discrete, fixed surface charges are assigned on the nanopore surface. The length of the pore is 31 Å, and the radius is 15 Å.

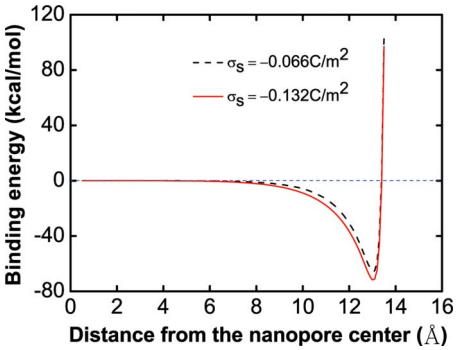

FIG. 2. (Color online) The binding energy for the Na^+ ion as a function of the distance from the nanopore center.

II. SIMULATION METHODS

Ionic current through a 3 nm in diameter nanopore was modeled for different concentration sodium chloride solutions under different surface charge densities using a modified TINKER 4.2 [24] molecular dynamics package. As shown in Fig. 1, the model system was composed of a 3 nm in diameter nanopore with periodical boundary conditions applied at each end of the nanopore. Discrete surface charges were distributed on the surface of the nanopore [11] and the model system was kept in electrical neutrality by initially setting the net charge number of counter ions and co-ions in the solution equal to the number of surface charges. About 1880 water molecules were included in the nanopore, which varied slightly for different cases because of the different number of ions in the nanopore. The water molecules were modeled using the SPC/E (extended simple point charge) model [25] and the intermolecular interactions were modeled by the summation of Lennard-Jones potentials and electrostatic potentials, which were processed by the Ewald summation algorithm [26].

The wall is qualitatively like the hydrophilic surface of silica, and the interactions between the surface and the fluid molecules are the same as those reported in the literature [27] using the Steele potential [28].

$$u_{wf}(r) = 2\pi\rho_w\varepsilon_{wf}\sigma_{wf}^2\Delta\left[\frac{2}{5}\left(\frac{\sigma_{wf}}{R-r}\right)^{10} - \left(\frac{\sigma_{wf}}{R-r}\right)^4 - \left(\frac{\sigma_{wf}^4}{3\Delta(R-r+0.61\Delta)^3}\right)\right], \quad (1)$$

where $\rho_w = 42.76$ nm^{-3} and $\Delta = 2.709$ Å. σ_{wf} and ε_{wf} are obtained from bulk silica parameters, $\varepsilon_w/k_B = 230$ K and $\sigma_w = 3.0$ Å, and the fluid molecular parameters by the Lorentz-Berthelot rules. R is the radius of the cylindrical tube and r is the distance of any molecule from the nanopore center. The interactions between the ions and the solid surface include contributions from the L-J potential and the electrostatic potential. The parameters for these potentials are the same as those in a previous publication [11]. The binding energy between an ion and the solid surface can be derived from the summation of the Lennard-Jones and the electrostatic potential. Figure 2 presents the binding energy profile between the Na^+ ions and the solid surface as a function of the distance from the nanopore center. In our modeling, the potential at $R = 0$ Å has been shifted to zero to reflect the zero potential in the center of the nanopore. Figure 2 shows that the optimal binding distance is approximately 2 Å away from the nanopore surface that is 15 Å away from the nanopore center and the binding energies are −65.5 and −71.6 kcal/mol corresponding to the cases with surface charge densities of −0.066 C/m^2 and −0.132 C/m^2, respectively. Due to the large binding energy of cations to the pore surface, it is observed that Na^+ ions could stay near the surface charge sites for the whole simulation period (4 ns), which indicates that the Na^+ residence time at the surface charge sites in our simulation can exceed (or be on the order of) 4 ns. Newton's equations of motion were integrated using the velocity Verlet algorithm with a time step of 2 fs. Berendsen thermostat [29] was used to keep the temperature at 298.0 K with a time constant of 0.1 ps. Only velocity components in the x and y directions were thermostated to not disturb the ion and fluid transport along the axial direction. To extract useful statistical information from the strong thermal background noise, the strongest electric field in the linear response regime was applied in the simulation. According to our study, the electric field of 1 V/nm is the upper limit of the linear response regime, which was applied along the axial (z-) direction of the nanopore to induce ionic current. The first 2 ns of the simulation was used to equilibrate the simulation system and then another 4 ns simulation was performed to extract the ionic current through the nanopore.

The ionic current is calculated by summing the net charges passing through a selected cross section in an interval as

$$I = \frac{\sum_j N_j q_j(\vec{n}\cdot\vec{z})}{\Delta t}, \quad (2)$$

where I is the ionic current; N_j is the net number of the j type ion passing through the fixed cross section during the interval Δt; q_j is the charge on the j type ion; $\vec{n}$ is a unit vector pointing to either the positive or negative z direction, representing the axial direction of the ion transport; and $\vec{z}$ is the unit vector of the z axis.

Even though it is well known that in nanochannels with overlapped electric double layers, neither the counter ion concentration nor the co-ion concentration will be that of the

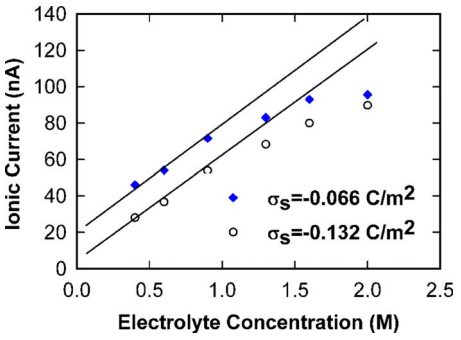

FIG. 3. (Color online) Ionic current as a function of the electrolyte concentration for surface charge densities of −0.066 and −0.132 C/m^2.

bulk electrolyte, there is no theory that can accurately predict the concentration of counter and co-ions in the nanochannels. It is a common practice in the literature of molecular dynamics simulation of electrokinetic phenomena to regard the co-ion concentration as the electrolyte concentration [30]. Here, we follow this practice and use the co-ion concentration to denote the electrolyte concentration.

III. RESULTS AND DISCUSSIONS

The effect of electrolyte concentration on ionic current was studied with two surface charge densities (σ_s): −0.066 C/m^2 and −0.132 C/m^2. Figure 3 shows the ionic current as a function of the electrolyte concentration from 0.4 to 2 M, which indicates that the ionic current increases almost linearly as the electrolyte concentration increases from 0.4 M to about 0.9 M, beyond which the increase deviates from linear to a significantly lower rate. The total number of mobile ions in the nanopore increases linearly with the electrolyte concentration, which should lead to linear ionic current increase, as when the electrolyte concentration increases from 0.4 to 0.9 M. However, for even higher electrolyte concentrations, the electric double layer becomes extremely thin. The highly packed counter ions in the thin near wall layer experience significantly larger viscous drag force from the wall, which leads to much lower mobility. The lower mobility at higher concentrations can be seen from the velocity profile of Na^+ ions, as shown in Fig. 4, which indicates that the velocity of the Na^+ ions decreases as the electrolyte concentration increases. To verify that the deviation from the linear trend in the concentration range of 0.9 to 2 M is truly because of the nanoscale channel, MD of bulk electrolyte was performed on a $3.2\times3.2\times3.2$ nm^3 simulation domain with periodic boundary conditions along the lateral directions (x and y directions) and 1 V/nm electric field in the z direction. The calculated electrical conductivity of the bulk electrolyte and that from the CRC Handbook [31] are plotted in Fig. 5. The calculated electrical conductivity fits that from the handbook very well, and both indicate that the electrical conductivity, and hence the electrical current, should increase approximately linearly with the electrolyte concentration in bulk solution till 2 M.

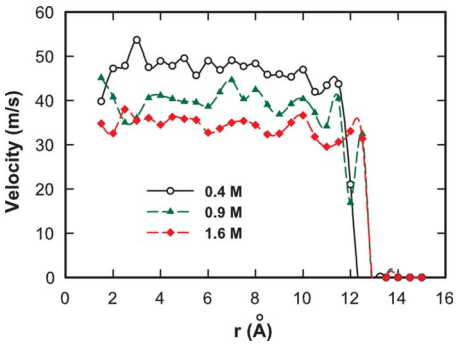

FIG. 4. (Color online) The Na^+ ion velocity profile for electrolyte concentrations of 0.4, 0.9, and 1.6 M.

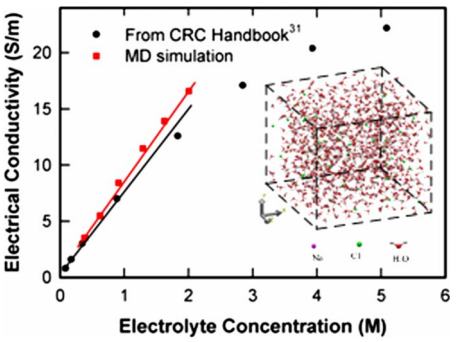

FIG. 5. (Color online) The electrical conductivity of bulk NaCl electrolyte versus molar concentration from MD simulation and CRC handbook [31]. The lines in the figure are drawn to guide eyes and the inset shows the simulation system for bulk electrolyte.

Compared to the nonlinearity of the ionic current at concentrations beyond 0.9 M, a more unexpected observation from Fig. 3 is that under the same concentration, the ionic current is always higher for a surface charge density of −0.066 C/m^2 than that of −0.132 C/m^2. It is well known that for higher surface charge densities, more mobile counter ions exist in a nanopore to balance the surface charges. Therefore, one would expect that the ionic current should be higher for higher surface charge densities, as suggested by the published reports on ionic current through nanochannels of tens of nanometers in diameter [6–8]. To further understand this unexpected result, we modeled the ionic current as a function of surface charge density at three electrolyte concentrations and the results are shown in Fig. 6.

Figure 6 shows that at the same concentration, the ionic current first increases with the surface charge density, a trend the same as that reported in the literature, which can be attributed to the increased number of mobile counter ions in the nanochannel. However, above certain critical value, the ionic current starts to decline as the surface-charge density further increases. This increase-decrease trend is the same for all three electrolyte concentrations (0.6, 1.3, and 2.0 M) calculated but more significant at lower electrolyte concentration. To further understand the contributions of the counter-ion (Na^+) and the co-ion (Cl^-) to the total ionic current, Fig. 7 presents the ionic currents calculated based on Na^+ ions and Cl^- ions at 0.6 M electrolyte concentration, the sum of which gives the total ionic current. It can be seen from Fig. 7 that the Na^+ current follows an increase-decrease

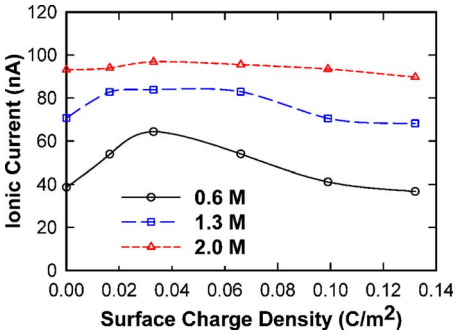

FIG. 6. (Color online) Ionic current as a function of the surface charge density for electrolyte concentrations of 0.6, 1.3, and 2 M.

profile while the Cl^- current follows an exactly opposite decrease-increase profile, which indicates that the increase-decrease profile for the total ionic current in Fig. 6 comes from the behavior of the Na^+ current. The Na^+ and Cl^- current at 1.3 and 2 M electrolyte concentrations shows similar profiles as those in Fig. 7.

We believe that the increase-decrease profile of the ionic current is the result of two competing effects: (1) the increasing number of counter ions in the nanopore to meet the charge neutrality requirement as the surface charge density increases, which tends to increase the ionic current; and (2) the lower mobility of the counter ions as the surface charge density increases, which tends to reduce the ionic current. The lower mobility at higher surface charge density comes from the fact that at high-surface charge density, more counter-ions are attracted to the near wall region, and experience larger viscous force. To verify this, we draw the distribution profile of Na^+ at different surface charge density and the velocity of the Na^+ ions across the nanopore cross section, as shown in Fig. 8. Figure 8(a) shows the number density of Na^+ ions, which is calculated by dividing the nanochannel into 30 layers along the radial direction and solving for the statistical number of Na^+ ions per unit volume in each layer. The number density distribution indicates that as the surface charge density increases, more counter ions are attracted to the first peak close to the nanopore surface. As a consequence, the velocities of the Na^+ ions decrease at high-

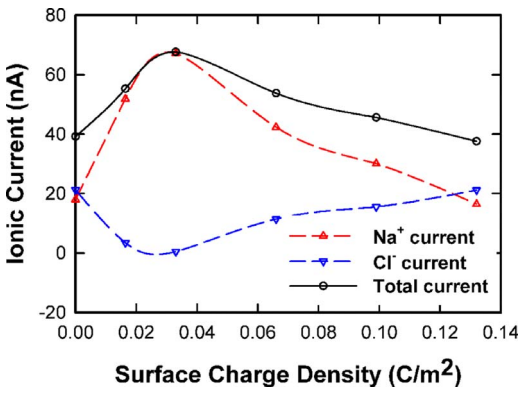

FIG. 7. (Color online) Contributions of Na^+ and Cl^- ions to the ionic current for 0.6 M NaCl solution under different surface charge densities.

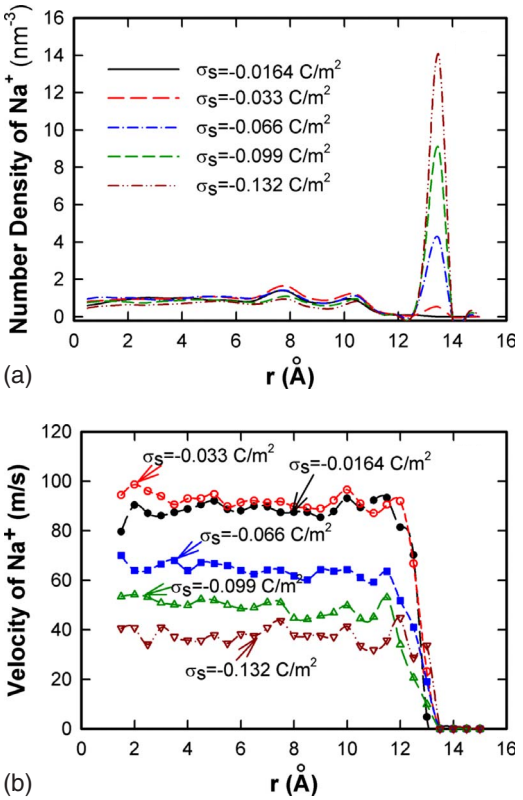

FIG. 8. (Color online) (a) The distribution and (b) the velocity profile of Na^+ ions in 0.6 M NaCl solution under different surface charge densities.

surface charge density, as shown in Fig. 8(b). Figure 8 supports our explanation that the decreasing profile at high-surface charge densities is the result of the lower mobility of the counter ions (Na^+) as the surface charge density increases.

The opposite decrease-increase profile of the co-ions (Cl^-) can be explained by the competing effects of the electrophoretic motion and the electroosmotic flow of the Cl^- ions. The electroosmotic flow first becomes stronger as the surface-charge density increases because of the increased zeta potential associated with the increased surface charge density; however, above the critical value, the reduced mobility of the counter ions becomes more dominant and the electroosmotic flow weakens. Since the electroosmotic flow is in the opposite direction of the electrophoretic motion of the Cl^- ions, the calculated Cl^- current first decreases and then increases.

It is worth noting that we believe the observed unexpected ionic current variation with the electrolyte concentration and the surface charge density can be true only in nanochannels of nanometer diameter. To observe the results, it requires that the contribution to the ionic current from the very thin near wall region to be comparable to or larger than that from the nanopore center region. This is because the observation is due to the ion mobility reduction, which occurs in the thin near wall region and to see the effects of this mobility reduction, it requires that the total number of ions in the near wall region to be comparable to or larger than that in the nanopore center. Therefore, the phenomenon will not be able to be

observed with nanochannels of tens of nanometers in diameter where the total number of ions in the channel center will be always higher than that in the thin near wall region. It is also worth noting that to what extent molecular dynamics results reflect reality depends on the level that the intermolecular interactions used in the simulation approach the true interactions. Therefore, it is important to experimentally verify the interesting phenomena we observed with the molecular dynamics simulation.

IV. SUMMARY

In summary, we applied molecule dynamics to study the ionic current of different concentration NaCl solutions through a 3 nm in diameter nanopore with different surface charge densities. Results show that for nanopores of this size, surface effects can lead to phenomena such as (1) nonlinear increase in ionic current with the electrolyte concentration as the electrolyte concentrations is higher than 0.9 M; and (2) the ionic current varies nonmonotonically as the surface charge density increases. These phenomena indicate that ion transport in nanopore deviates from the bulk behavior even at high-electrolyte concentration with nonoverlapped electric double layers. Specifically, contrary to the common understanding, even the total number of mobile ions in the nanopore increases, the ionic current can decrease because of the strong boundary effects.

ACKNOWLEDGMENTS

Y.G. and Y.C. thank the support from the National Basic Research Program of China (Grant No. 2006CB300404), National Natural Science Foundation of China (Grants No. 50676019 and No. 50875047), and the Natural Science Foundation of Jiangsu Province through Grants No. BK2006510 and No. BK2007113. D.X. and D.L. acknowledge the financial support from the U.S. National Science Foundation (Grant No. CBET-0643583). The molecular dynamics simulation was performed using the Vanderbilt Advanced Computing Center for Research and Education (ACCRE).

[1] J. J. Kasianowicz, E. Brandin, D. Branton, and D. W. Deamer, Proc. Natl. Acad. Sci. U.S.A. **93**, 13770 (1996).
[2] J. Li, D. Stein, C. McMullan, D. Branton, M. J. Aziz, and J. A. Golovchenko, Nature (London) **412**, 166 (2001).
[3] H. Chang, F. Kosari, G. Andreadakis, M. A. Alam, G. Vasmatzis, and R. Bashir, Nano Lett. **4**, 1551 (2004).
[4] R. M. M. Smeets, U. F. Keyser, D. Krapf, M. Y. Wu, N. H. Dekker, and C. Dekker, Nano Lett. **6**, 89 (2006).
[5] R. R. Henriquez, T. Ito, L. Sun, and R. M. Crooks, Analyst **129**, 478 (2004).
[6] D. Stein, M. Kruithof, and C. Dekker, Phys. Rev. Lett. **93**, 035901 (2004).
[7] H. Daiguji, P. Yang, and A. Majumdar, Nano Lett. **4**, 137 (2004).
[8] R. Karnik, R. Fan, M. Yue, D. Li, P. Yang, and A. Majumdar, Nano Lett. **5**, 943 (2005).
[9] R. B. Schoch and P. Renaud, Appl. Phys. Lett. **86**, 253111 (2005).
[10] W. Zhu, S. Singer, Z. Zheng, and A. Conlisk, Phys. Rev. E **71**, 041501 (2005).
[11] Y. Chen, Z. Ni, G. Wang, D. Xu, and D. Li, Nano Lett. **8**, 42 (2008).
[12] R. Qiao and N. R. Aluru, J. Chem. Phys. **118**, 4692 (2003).
[13] J. Cervera, B. Schiedt, R. Neumann, S. Mafé, and P. Ramı'rez, J. Chem. Phys. **124**, 104706 (2006).
[14] D. Krapf, B. M. Quinn, M. Y. Wu, H. W. Zandbergen, C. Dekker, and S. G. Lemay, Nano Lett. **6**, 2531 (2006).
[15] E. R. Cruz-Chu, A. Aksimentiev, and K. Schulten, J. Phys. Chem. C **113**, 1850 (2009).
[16] K. Leung, S. B. Rempe, and C. D. Lorenz, Phys. Rev. Lett. **96**, 095504 (2006).
[17] C. D. Lorenz and T. Travesset, Phys. Rev. E **75**, 061202 (2007).
[18] J. Dzubiella and J.-P. Hansen, J. Chem. Phys. **122**, 234706 (2005).
[19] C. Peter and G. Hummer, Biophys. J. **89**, 2222 (2005).
[20] L. Yang and S. Garde, J. Chem. Phys. **126**, 084706 (2007).
[21] K. Leung, J. Am. Chem. Soc. **130**, 1808 (2008).
[22] B. Corry, J. Phys. Chem. B **112**, 1427 (2008).
[23] S. Joseph and N. R. Aluru, Nano Lett. **8**, 452 (2008).
[24] J. W. Ponder, *TINKER–Software Tools for Molecular Design, User's Guide for Version 4.2* (Washington University School of Medicine, St. Louis, MO, 2004).
[25] H. J. C. Berendsen, J. R. Grigera, and T. P. Straatsma, J. Phys. Chem. **91**, 6269 (1987).
[26] A. Bródka and P. Śliwiński, J. Chem. Phys. **120**, 5518 (2004).
[27] S. T. Cui and H. D. Cochran, J. Chem. Phys. **117**, 5850 (2002).
[28] W. A. Steele, Surf. Sci. **36**, 317 (1973).
[29] H. J. C. Berendsen, J. P. M. Postma, W. F. van Gunsteren, A. DiNola, and J. R. Haak, J. Chem. Phys. **81**, 3684 (1984).
[30] R. Qiao and N. R. Aluru, Phys. Rev. Lett. **92**, 198301 (2004).
[31] *CRC Handbook of Chemistry and Physics, 89th Edition (Internet Version 2009)*, edited by David R. Lide (CRC Press/Taylor and Francis, Boca Raton, FL, 2009).